https://doi.org/10.1016/j.enbuild.2017.01.073



# A Dynamic Dehumidifier Model for Simulations and Control of Liquid Desiccant Hybrid Air Conditioning Systems

Lingshi Wang[1], Fu Xiao[1,*], Xiaofeng Niu[2], Dian-ce Gao[1]

[1]*Department of Building Services Engineering, The Hong Kong Polytechnic University, Kowloon, Hong Kong*
[2]*College of Urban Construction, Nanjing Tech University, Nanjing 210009, China*

*****Corresponding author. Tel.: +852 2766 4194; Fax: +852 2765 7198.

*E-mail address*: linda.xiao@polyu.edu.hk

## ABSTRACT

Liquid desiccant (LD) dehumidification has attracted increasing attentions and its applications in air conditioning are emerging in recent years. The dynamic characteristics of the dehumidifier are essential to design and tune controllers for LD hybrid air conditioning systems. Existing research on liquid desiccant dehumidifier focuses on steady state condition. There is a lack of a computationally efficient yet accurate dynamic dehumidifier model for the purpose of control and dynamic simulations. This study develops a simplified one-dimensional dynamic model of a counter flow packed-type dehumidifier. The approach to quantifying the thermal mass of packing material and desiccant solution held in dehumidifier is developed for the first time and implemented in the dynamic model. Validation results show that the dynamic model is in better agreement with experiment than the static model. Root-Mean-Square Errors (RMSEs) between the simulation results of dynamic model and the experimental results are about 0.2g/kg for the outlet air humidity ratio and 0.2°C for the outlet air temperature. In addition, sensitivity analysis is conducted to investigate the effects of the thermal mass on the dehumidifier dynamics. The dynamic model and the results are valuable to design and tune controllers and dynamic simulations of the LD hybrid air conditioning systems.

*Keywords*: Liquid desiccant dehumidifier; Dynamic model; Thermal mass; Time constant; Heat and mass transfer

**Nomenclature**

| | |
|---|---|
| $a$ | specific surface area of packing ($m^2/m^3$) |
| $a_w$ | wetted specific surface area of packing($m^2/m^3$) |
| $A$ | cross sectional area of packing ($m^2$) |
| $c$ | specific heat capacity (kJ/(kg $^oC$)) |
| $C$ | heat capacity (kJ/ $^oC$) |
| C1- C4 | parameters in the dynamic model |
| $d_e$ | equivalent diameter (mm) |
| $D_a$ | diffusion coefficient of water vapor in air ($m^2/s$) |
| $G$ | mass flow flux of air ($kg/m^2s$) |
| $h$ | specific enthalpy (kJ/kg) |
| $H$ | height of packing (m) |
| $k_a$ | heat transfer coefficient (kW/($m^2$ $^oC$)) |
| $k_m$ | mass transfer coefficient (kg/($m^2$ s)) |
| $L$ | mass flow flux of desiccant ($kg/m^2s$) |
| $Le$ | Lewis number |
| $m$ | mass flow rate (kg/s) |
| $m_{de}$ | dehumidification rate (g/s) |
| $M_a$ | mass of air in the dehumidifier (kg) |
| $M_{dy}$ | mass of dynamic desiccant solution held in the dehumidifier (kg) |
| $M_p$ | dry weight of the packing (kg) |
| $M_s$ | total mass of desiccant solution held in the dehumidifier (kg) |
| $M_{st}$ | mass of static desiccant solution held in the dehumidifier (kg) |
| $\overline{\boldsymbol{M}}_{\mathbf{dy}}$ | mass of dynamic desiccant held by unit volume of packing ($kg/m^3$) |
| $\overline{\boldsymbol{M}}_{\mathbf{st}}$ | mass of desiccant absorbed by unit mass of packing (kg/kg) |
| $MAE$ | Mean Absolute Error |
| $NTU$ | number of transfer units |
| $Nu$ | Nusselt number, $k_a a d_e^2/\lambda$ |
| $P$ | partial vapor pressure (Pa) |
| $P_0$ | partial vapor pressure of saturated water at 25$^o$C (Pa) |
| $Pr$ | Prandlt number |
| $r$ | latent heat of phase change (kJ/kg) |
| $Re$ | Reynolds number, $ud_e/v_a$ |
| $RMSE$ | Root-Mean-Square Error |
| $Sc$ | Schmidt number |
| $Sh$ | Sherwood number,$k_m a d_e^2/(D_a \rho_a)$ |
| $T$ | temperature ($^o$C) |
| $u$ | air velocity (m/s) |
| y | length of height direction (m) |

*Greek symbols*

| | |
|---|---|
| $\varepsilon$ | volume fraction in dehumidifier |
| $\xi$ | solution mass concentration (%) |
| $\rho$ | density ($kg/m^3$) |
| $\tau$ | time (s) |
| $\tau_c$ | time constant (s) |
| $v_a$ | kinematic viscosity of air ($m^2/s$) |
| $\eta$ | dehumidification effectiveness |
| $\omega$ | humidity ratio (g/kg) |
| λ | coefficient of thermal conductivity of air (W/(m $^o$C)) |

*Subscripts*

| | |
|---|---|
| a | air |
| e | equilibrium state |
| Exp | experimental value |
| in | inlet |
| max | maximum |
| min | minimum |
| Num | numerical value |
| out | outlet |
| p | packing |
| s | solution |
| w | wetted area |

## 1. Introduction

In conventional air-conditioning systems, the air dehumidification process consumes about 20-40% of the overall energy [1]. This ratio can be even higher on occasions when total fresh air ventilation is required [1]. The main reason for such high energy consumption is that the air has to be dehumidified by condensation at a very low temperature. The liquid desiccant dehumidification is a promising alternative method for removing moisture from the air. In this method, the moisture is absorbed from the air by the concentrated liquid desiccant solution at a room temperature. A higher chiller COP (Coefficient of Performance) and significant energy saving can be achieved by using liquid desiccant for air dehumidification [2-4]. In addition, the liquid desiccant dehumidification system can be driven by low-grade heat sources such as the solar energy or the waste heat [5, 6], which further contributes to energy conservation.

In recent years, researchers developed a diversity of liquid desiccant hybrid air conditioning systems [2-4, 7, 8] and commercial products of those hybrid systems are emerging [2, 9-11]. Control issues are becoming critical to the actual performance of the systems operating under dynamic conditions, including the changing outdoor weather conditions and indoor heating/cooling loads [10]. As some of the controllers in the hybrid systems directly control the inlet fluids of the dehumidifier, such as the inlet solution temperature or flow rate [7], the dynamic characteristics of the dehumidifier greatly affect the control performance. The dynamic characteristics of the coupled heat and mass transfer process occurring in the dehumidifier is crucial to the design of controllers and operation strategies. However, almost all existing research works on liquid desiccant systems focus on the analysis of their steady-state performance using steady-state models. Although optimal control of liquid desiccant based air-conditioning system has been studied [7, 8, 12], the dynamics of the dehumidification process was neglected and the steady-state model of the dehumidifier was used. For better understanding the dynamic characteristics of the dehumidifier and more realistic dynamic simulation involving real-time control, a computationally efficient yet reasonably accurate dynamic model of the dehumidifier is needed.

The dehumidifier is the major component in the liquid desiccant systems. The packed tower is a popular configuration of LD dehumidifiers. Many studies have been conducted on the heat and mass transfer models of the packed-type dehumidifiers. The existing mathematical models can be roughly divided into two categories: the finite difference model and the effectiveness-*NTU* model. The finite difference model is the detailed model composed of the heat and mass transfer differential equations. Treybal [13] proposed a heat and mass transfer differential equations model for an adiabatic dehumidifier. Khan and Ball [14], and Chen *et al*. [15] developed a new finite difference *Le-NTU* model. The analytical solution of the *Le-NTU* model was given by Chen *et al*. [15], and Liu *et al*. [16] for static system simulation. Another analytical solution for the *Le-NTU* model of dehumidifier was obtained by assuming that the equilibrium humidity ratio of the desiccant solution is constant during the dehumidification process [17]. In general, the finite difference model is solved by the numerical method and it is difficult to get the analytical solution. The effectiveness-*NTU* model is the simplified model developed for efficient calculations. Similar to the effectiveness model of a cooling tower, an effectiveness-*NTU* model of a dehumidifier was developed by Stevens *et al*. [18]. Wang *et al*. [19] proposed a hybrid steady-state model with lumped parameters which can be determined through identification to predict the heat and mass transfer rate in a packed-type dehumidifier. No iterative calculations are required and the equations involved are easy to be solved. The above-mentioned steady-state models were usually used for the performance analysis, configuration optimization of dehumidifier and hybrid system optimization [7, 8, 15, 19].

Very limited studies related to the dynamic modelling of the liquid desiccant dehumidification process can be found from open resources. One relevant literature is from Peng and Pan's work [20]. They developed one-dimensional non-equilibrium heat and mass transfer model of a counter flow packed-type dehumidifier. This model was a detailed model considering the heat conduction and mass diffusion effects. It was specifically developed for characterizing the dynamic performance of the dehumidifier under the condition of low desiccant flow velocity ($2.4\times10^{-4}$ m/s). The normal desiccant velocities used in other research and practical applications are much higher than that in Peng's study. It is because low desiccant flow velocity may result in a large increase in the solution temperature and decrease in the solution concentration, which significantly deteriorates the dehumidification capability. In addition, Namvar *et al.* developed a two-dimensional transient mathematical model of a liquid-to-air counter-cross flow semi-permeable membrane energy exchangers [21]. The thermal mass of the panels and shell which significantly influences the dynamic response of the exchanger was considered in the model. Using the model, the authors studied the time constants under different operating conditions. Luo *et al.* [22] simulated the unsteady desiccant film flow along a flat plate using the CFD software FLUENT. It is well known that the CFD calculation is timeconsuming, which is not suitable for system dynamic simulation. There is a lack of a computationally efficient dynamic model of the liquid desiccant dehumidifier.

One of the major challenges to dynamic modelling of the liquid desiccant dehumidifier is to quantify the thermal mass of the packing and the desiccant solution held in the dehumidifier, which may significantly delay the heat and mass transfer process. To capture the dynamic characteristics of the dehumidification process, the model should incorporate sufficient physical meanings, which means the black-box models like the neural networks and the data-driven models are not suitable. For the purpose of dynamic simulation of the hybrid system involving real-time control, the dynamic model should be computationally efficient. Therefore, too detailed physical models are not desired which usually require detailed configuration parameters and properties, and consume substantial computation time. This paper develops and validates a simplified one-dimensional dynamic model of a counter flow packed-type dehumidifier based on the control volume analysis method. Thermal mass of the packing and the desiccant solution held in the dehumidifier are properly quantified and introduced into the dynamic model. The determination of the heat and mass transfer coefficients or the Lewis number is also a big challenge. In most research on static models of the dehumidifier, the Levis number was assumed to be 1 [16]. This paper develops new correlations of the heat and mass transfer coefficients. The model is validated experimentally under different dynamic working conditions. The effects of the dehumidifier thermal mass on the time constants of the heat and mass transfer process are analyzed using the model. Compared with the existing models, the proposed model is simple and accurate which is suitable for dynamic simulation and real-time control of the liquid desiccant based air conditioning equipment.

## 2. Mathematical model

The mathematical model is developed to characterize the dynamic heat and mass transfer characteristics of the liquid desiccant dehumidification process in a packed-type dehumidifier. The counter flow pattern is employed between the air and the desiccant solution. The air flows from the bottom to the top of the dehumidifier and the desiccant solution is spread at the top of the packing and flows down along the packing. The schematic of the heat and mass transfer process in a typical counter flow packed-type dehumidifier is shown in Fig.1.

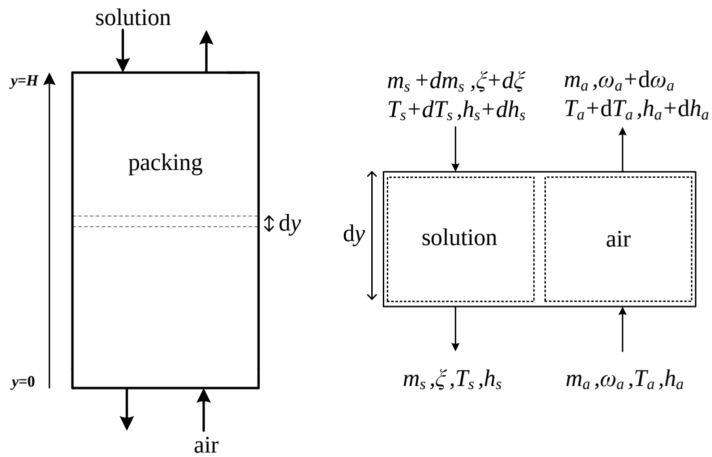


Fig. 1. Schematic of heat and mass transfer process in a counter flow packed-type dehumidifier.

Most of the previous steady-state models didn't consider the thermal mass of the packing material and the desiccant solution held in the dehumidifier. In dynamic modeling, they cannot be ignored. The packing materials themselves can store or release heat during the dynamic process. Some packing materials, such as the porous materials, can absorb a quite large amount of solution [23]. Meanwhile, part of the desiccant solution may be attached on the surface of the packing to form a thin film which also influences the dynamic process. It is a big challenge to quantify the amount of solution held in the dehumidifier [24, 25]. This study recommends convenient approaches to quantifying the thermal mass of the packing material and the desiccant solution held in the dehumidifier using the properties of the packing material, configuration parameters of the packing from manufacturers as well as simple tests. Details are given in the section of determination of parameters in the model.

### *2.1. Assumptions*

To simplify dynamic heat and mass transfer analysis, several basic assumptions are made as follows:

(1) The process of heat and mass transfer is one dimensional unsteady state along the flow direction.

(2) Lumped parameter method is applied to each control volume. There is no temperature gradient in the interior of the control volume.

(3) Heat conduction and molecular diffusion among the air, solution and packing are negligible.

(4) The packing is considered thermal equilibrium with the desiccant solution. Thus, the packing temperature

is assumed to be equal the contacted solution temperature ($T_{\mathrm{p}} = T_{\mathrm{s}}$) when the desiccant solution flows through the packing.

(5) In the dehumidification process, the latent heat of water vapor condensation is fully absorbed by the solution.

(6) The dehumidifier is adiabatic with the surroundings.

Detailed explanations for some of the above assumptions are offered as follows.

For the first assumption, as the cross section of packing is usually square or circular, which is symmetric and it appears similar state for air or solution on the whole cross section. So, the distributions of the fluid states on one certain cross section can be assumed to be even.

For the second assumption, the major requirement for applying the lumped parameter method is that the Biot (*Bi*) number is less than 0.1. In the packed-type dehumidifier, both the thickness of the desiccant film and the dimension of the control volume are very small. The heat transfer coefficient is also low due to the low air flow velocity. Therefore, the lumped parameter method can be used in this study.

For the third assumption, the heat conduction and the molecular diffusion are neglected because the heat convection is dominant during the dehumidification process in the counter flow packed-type dehumidifier. However, when the desiccant solution flow velocity is extremely slow, the heat conduction and molecular diffusion should be considered [20].

For the fifth assumption, the latent heat of water vapor condensation is assumed to be fully absorbed by the desiccant solution because the convective heat and mass transfer coefficients on the air side are usually much smaller than that on the liquid side [26].

### *2.2. Model development*

#### *2.2.1. Dynamic heat and mass transfer model*

The control volume analysis method is employed to develop the dynamic heat and mass transfer model of the dehumidification process. The dehumidifier can be divided into a number of control volumes along the flow direction. Based on the assumptions, the control volume can be divided into two sides: the air side, the solution and packing side, respectively. The control volume analysis, including the heat balance analysis and the mass balance analysis, is conducted for the two sides, respectively. The schematic of the control volume analysis is shown in Fig.2.

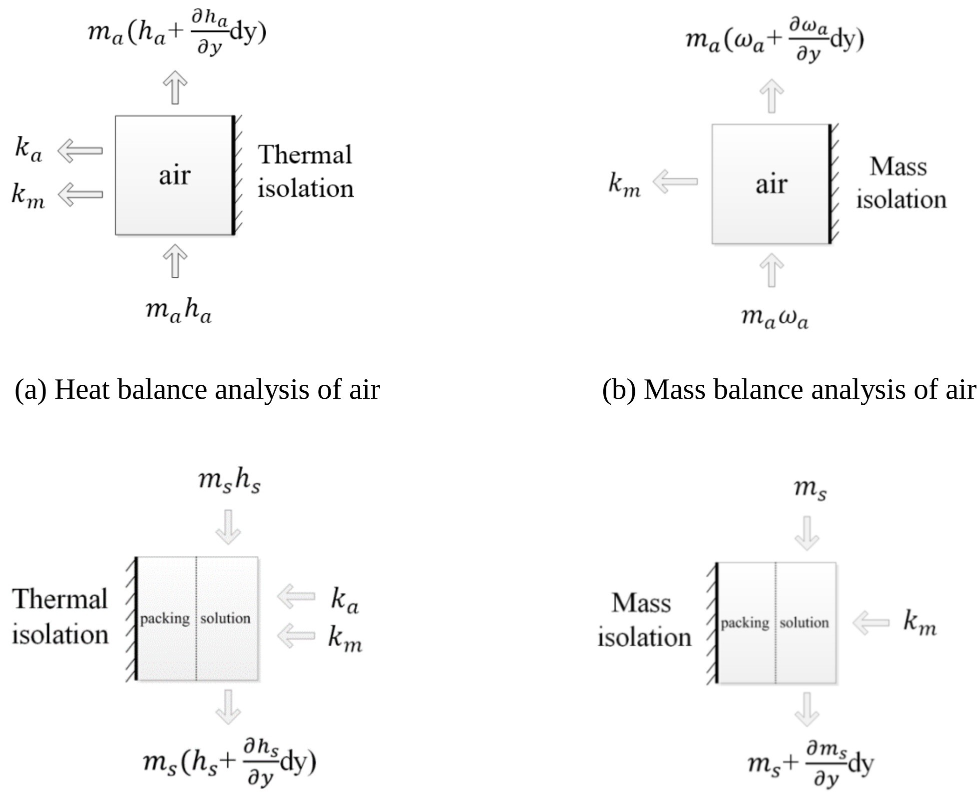


(a) Heat balance analysis of air

(b) Mass balance analysis of air

(c) Heat balance analysis of solution and packing

(d) Mass balance analysis of solution and packing

Fig. 2. Control volume analysis of heat and mass transfer processes.

Air energy conservation equation:

$$\varepsilon_{\mathrm{a}}\, A\, dy\, \rho_{\mathrm{a}}\, \frac{\partial h_{\mathrm{a}}}{\partial \tau} = k_{\mathrm{a}}\, a_{\mathrm{w}}\, A\, dy(T_{\mathrm{s}} - T_{\mathrm{a}}) - m_{\mathrm{a}}\, \frac{\partial h_{\mathrm{a}}}{\partial y} dy - k_{\mathrm{m}}\, a_{\mathrm{w}}\, A\, dy(\omega_{\mathrm{a}} - \omega_{\mathrm{e}})\, r \tag{1}$$

Air mass conservation equation:

$$\varepsilon_{\mathrm{a}}\, A\, dy\, \rho_{\mathrm{a}}\, \frac{\partial \omega_{\mathrm{a}}}{\partial \tau} = -k_{\mathrm{m}}\, a_{\mathrm{w}}\, A\, dy(\omega_{\mathrm{a}} - \omega_{\mathrm{e}}) - m_{\mathrm{a}}\, \frac{\partial \omega_{\mathrm{a}}}{\partial y} dy \tag{2}$$

Solution and packing energy conservation equation:

$$(\varepsilon_{\mathrm{s}} A\, dy\, \rho_{\mathrm{s}} c_{\mathrm{s}} + \varepsilon_{\mathrm{p}}\, A\, dy\, \rho_{\mathrm{p}} c_{\mathrm{p}})\, \frac{\partial T_{\mathrm{s}}}{\partial \tau} = -k_{\mathrm{a}}\, a_{\mathrm{w}}\, A\, dy(T_{\mathrm{s}} - T_{\mathrm{a}}) + \frac{\partial (m_{\mathrm{s}} h_{\mathrm{s}})}{\partial y} dy + k_{\mathrm{m}}\, a_{\mathrm{w}}\, A\, dy(\omega_{\mathrm{a}} - \omega_{\mathrm{e}})\, r \tag{3}$$

Solution and packing mass conservation equation:

$$\frac{\varepsilon_{\mathrm{s}}\, A\, dy \rho_{\mathrm{s}}}{m_{\mathrm{s,in}}}\frac{\partial m_{\mathrm{s}}}{\partial \tau} = k_{\mathrm{m}}\, a_{\mathrm{w}}\, A\, dy(\omega_{\mathrm{a}} - \omega_{\mathrm{e}}) + \frac{\partial m_{\mathrm{s}}}{\partial y} dy \tag{4}$$

where, $\omega_{\mathrm{a}}$, $T_{\mathrm{a}}$, $h_{\mathrm{a}}$, $m_{\mathrm{a}}$ are the humidity ratio, temperature, specific enthalpy and mass flow rate of the air, respectively; $T_{\mathrm{s}}$, $h_{\mathrm{s}}$, $m_{\mathrm{s}}$ are the temperature, specific enthalpy and mass flow rate of the desiccant solution, respectively; $\omega_{\mathrm{e}}$ is the equivalent humidity ratio of desiccant solution based on the water vapor partial pressure of the desiccant solution surface, and the water vapor partial pressure can be calculated by the temperature and concentration of the desiccant solution; $a_{\mathrm{w}}$ is the wetted specific surface area for heat and mass transfer; $\varepsilon_{\mathrm{a}}$, $\varepsilon_{\mathrm{s}}$, $\varepsilon_{\mathrm{p}}$ are the volume fractions of air, solution and packing in the dehumidifier, respectively; $k_{\mathrm{a}}$ and $k_{\mathrm{m}}$ are the heat and mass transfer coefficients between the air and the desiccant solution, respectively; $r$ is the latent heat of phase change.

As mentioned earlier, the *Le-NTU* equations have been developed for the steady-state finite difference model in the previous studies [14, 15]. In this study, *Le-NTU* equations for the dynamic finite difference model of the dehumidifier are developed in a similar way. Firstly, Lewis (*Le*) number and *NTU* are defined as Eqs. (5) and (6).

$$Le = \frac{k_{\mathrm{a}}}{k_{\mathrm{m}}\, c_{\mathrm{a}}} \tag{5}$$

$$NTU = \frac{k_{\mathrm{m}}\, a_{\mathrm{w}}\, A\, H}{m_{\mathrm{a}}} \tag{6}$$

Combining Eqs. (1) and (2), the specific enthalpy equation of air can be derived as in Eq. (7). Based on Eq. (2), the humidity ratio equation of air can be derived as Eq. (8). Combining Eqs. (1) and (3), the specific enthalpy equation of solution can be derived as Eq. (9). Combining Eqs. (2) and (4), the mass flow rate equation of solution can be derived as Eq. (10).

$$\frac{\partial h_{\mathrm{a}}}{\partial \tau} = \mathrm{C1}\ \left\{\frac{NTU}{H}\left[Le(h_{\mathrm{e}} - h_{\mathrm{a}}) + (1 - Le)\ r\ (\omega_{\mathrm{e}} - \omega_{\mathrm{a}})\right] - \frac{\partial h_{\mathrm{a}}}{\partial y}\right\} \tag{7}$$

$$\frac{\partial \omega_{\mathrm{a}}}{\partial \tau} = \mathrm{C1}\ \left\{\frac{NTU}{H}(\omega_{\mathrm{e}} - \omega_{\mathrm{a}}) - \frac{\partial \omega_{\mathrm{a}}}{\partial y}\right\} \tag{8}$$

$$\mathrm{C2}\frac{\partial h_{\mathrm{s}}}{\partial \tau}+\mathrm{C3}\ \frac{\partial h_{\mathrm{a}}}{\partial \tau}\ =\frac{\partial (m_{\mathrm{s}}\,h_{\mathrm{s}})}{\partial y}-m_{\mathrm{a}}\frac{\partial h_{\mathrm{a}}}{\partial y} \tag{9}$$

$$\mathrm{C4}\ \frac{\partial m_{\mathrm{s}}}{\partial \tau}+\mathrm{C3}\ \frac{\partial \omega_{\mathrm{a}}}{\partial \tau}\ =\frac{\partial m_{\mathrm{s}}}{\partial y}-m_{\mathrm{a}}\ \frac{\partial \omega_{\mathrm{a}}}{\partial y} \tag{10}$$

where,

$$\mathrm{C1}=\frac{m_{\mathrm{a}}H}{M_{\mathrm{a}}}$$

$$\mathrm{C2}=\frac{M_{\mathrm{s}}+\frac{c_{\mathrm{p}}}{c_{\mathrm{s}}}M_{\mathrm{p}}}{H}$$

$$\mathrm{C3}=\frac{M_{\mathrm{a}}}{H}$$

$$\mathrm{C4}=\frac{M_{\mathrm{s}}}{m_{\mathrm{s,in}}\,H}$$

$h_e$ is the air specific enthalpy in equilibrium with the desiccant solution; $M_a$ is the air mass in the dehumidifier; $M_s$ is the total mass of desiccant solution held in the dehumidifier [27]; $M_p$ is dry weight of the packing. $M_a$, $M_s$ and $M_p$ represents the thermal mass of the air, the desiccant solution held in the dehumidifier and the packing in the dehumidifier, respectively.

Eqs. (7) - (10) are the dynamic heat and mass transfer model of the dehumidifier. The dynamic air states (including $h_{\mathrm{a}}$ and $\omega_{\mathrm{a}}$) and the dynamic desiccant solution states (including $h_{\mathrm{s}}$ and $m_{\mathrm{s}}$) of each control volume can be obtained by solving the dynamic model.

It is noted that the left sides of Eqs. (7) - (10) will become zero if the dynamic heat and mass transfer process reaches the steady state. In this case, the proposed dynamic equations converge to steady-state equations mentioned in [15]. It shows one of the critical issues in dynamic modelling is to determine the values of C1-C4 in the left sides of the equations, i.e. the thermal mass of each component.

### *2.2.2. Boundary and initial conditions*

The initial conditions and boundary conditions are set as follows:

Initial conditions:

$$\tau = 0:\quad T_a = T_p = T_{a,in}\ ,\ \omega_a = \omega_{a,in}\ ,\ \ m_s = 0 \tag{11}$$

Boundary conditions:

$$y=0: \quad T_a = T_{a,in}\ ,\ \omega_a = \omega_{a,in}\ ,\ \frac{\partial T_s}{\partial y} = 0\ ,\ \frac{\partial \xi}{\partial y} = 0\ ,\ \frac{\partial m_s}{\partial y} = 0 \tag{12}$$

$$y=H: \quad T_s = T_p = T_{s,in}\ ,\ m_s = m_{s,in}\ ,\ \xi = \xi_{in}\ ,\ \frac{\partial T_a}{\partial y} = 0\ ,\ \frac{\partial \omega_a}{\partial y} = 0 \tag{13}$$

In Eq. (13), $T_{s,in}$ is the measured solution temperature located at the inlet of the dehumidifier. In real applications, the solution temperature ($T_s$) located at the top of the packing is approximately equal to $T_{s,in}$ when the inlet desiccant temperature is stable or changes slowly. However, when the inlet solution temperature changes fast, $T_s$ is hardly equal to $T_{s,in}$ because there is a small amount of desiccant remaining in the spray heads and distributors over the packing. In this case, $T_s$ can be estimated by considering the small amount of the desiccant solution stored in the spray headers as a heat capacity through Eq. (14).

$$C\frac{dT_s}{d\tau} = m_s c_s (T_{s,in} - T_s) \tag{14}$$

where, $T_{s,in}$ is the desiccant temperature at the inlet of the dehumidifier; $T_s$ is the desiccant temperature leaving the spray headers.

### *2.2.3. Numerical solution*

The proposed dynamic model of the liquid desiccant dehumidifier consists of four partial differential equations, which is difficult to get the analytical solution. In this research, the numerical method is employed to solve the equations. The differential equations (7) - (10) are discretized using the finite difference method. The packing is divided into *N* sections from bottom to top. The derivatives with respect to the time variables are estimated using an implicit scheme. The space variables are estimated using a first-order upwind scheme. FORTRAN language is utilized for programming. Numerical solution is finally obtained using the iterative method. Fig.3 shows the flow chart for the numerical solution of the dynamic model.

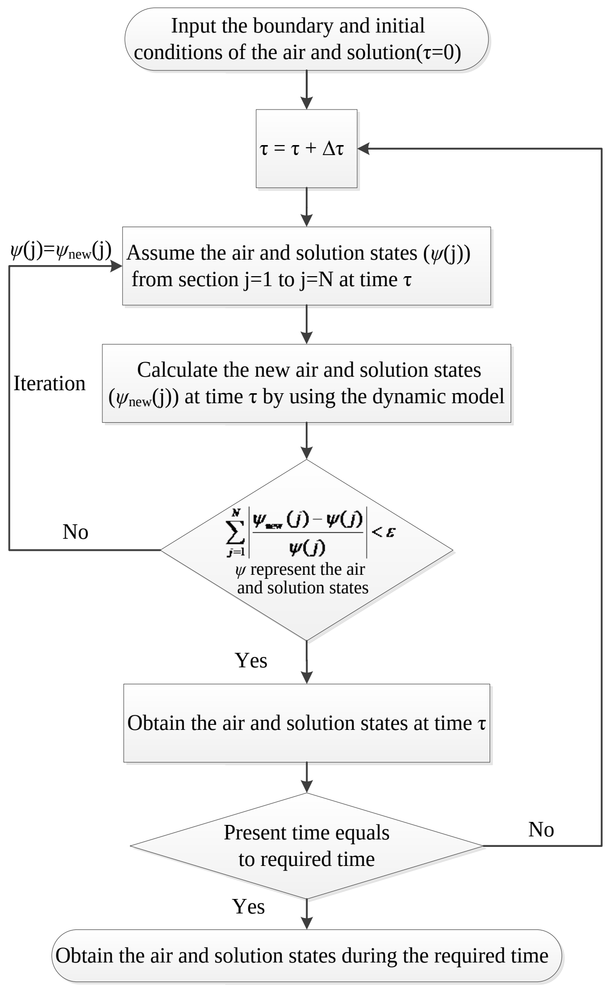


Fig. 3. Flow chart for the numerical solution of the dynamic model.

*2.3. Determination of parameters in the model*

Six unknown parameters in the proposed model need to be determined, which including C1-C4 as well as *NTU* and Lewis number.

Parameters C1-C4 can be calculated from the unknown parameters $M_p$, $M_s$ and $M_a$. $M_p$ is the dry weight of the packing which can be determined from the density of the packing material, the dimensions and the volume fraction of the packing, as shown in Eq. (15).

$$M_{\mathrm{p}} = \rho_{\mathrm{p}}\varepsilon_{\mathrm{p}}AH \tag{15}$$

where, *A* is the cross sectional area of the packing and *H* is the height of the packing. The densities of some typical packing materials are: polypropylene 0.91g/cm$^3$, ceramic 2.5g/cm$^3$, stainless steel 7.9g/cm$^3$. The volume fraction is the volume ratio of the packing material and the packed tower. It can be determined by the void fraction of the packing, which is usually provided by the manufacture of the packing.

$M_s$ refers to the total mass of desiccant solution held in the dehumidifier which comprises static ($M_{st}$) and dynamic ($M_{dy}$) components [25], as show in Eq. (16).

$$M_{\mathrm{s}} = M_{\mathrm{st}} + M_{\mathrm{dy}} \tag{16}$$

The mass of static desiccant solution ($M_{st}$) held in the dehumidifier represents the mass of the solution absorbed by the packing material which will hardly leave the packing when the solution supply is stopped. However, the mass of dynamic desiccant solution ($M_{dy}$) represents the mass of the solution attached on the surface of the packing which will leave the packing soon after the solution supply is stopped.

Al-Farayedhi *et al.* [27] and Rocha *et al.* [24] adopted the similar definitions of $M_{st}$ and $M_{dy}$ for metal structured packings. In their studies, $M_{st}$ was nearly equal to zero because the packing was made of metal which hardly absorbs any solution. For the packing made of other materials which can absorb desiccant solution, $M_{st}$ can be calculated by Eq. (17).

$$M_{\mathrm{st}} = \rho_{\mathrm{p}} \varepsilon_{\mathrm{p}} A H \overline{M}_{\mathrm{st}} \tag{17}$$

In Eq. (17), $\overline{M}_{\mathrm{st}}$ is the mass of the desiccant solution absorbed by the unit mass of packing material, which only depends on the properties of packing material for given desiccant solution. $\overline{M}_{\mathrm{st}}$ is usually available from the packing manufacturer. For example, one kilogram CELdek packing material can absorb 1.608 kilograms LiCl solution, i.e. $\overline{M}_{\mathrm{st}}$ is equal to 1.608. In case this value is not available from manufacture, it is also convenient to get this value by weighing a piece of packing material before and after soaking it in the solution.

$M_{dy}$ can be calculated by Eq. (18), in which $\overline{M}_{\mathrm{dy}}$ is the mass of desiccant solution attached on unit volume of packing. $\overline{M}_{\mathrm{dy}}$ is influenced by the configuration of packing, the viscosity and surface tension as well as the mass flow flux ($L$) of solution [24]. $L$ is the mass flow rate of solution per unit cross sectional area of packing. When the types of the packing and the desiccant solution are given, $\overline{M}_{\mathrm{dy}}$ is only influenced by the mass flow flux of solution. It is convenient to determine $\overline{M}_{\mathrm{dy}}$ using the conventional volumetric method [28], i.e. measuring the amount of the solution leaving the packing after the solution supply is stopped. The expression of $\overline{M}_{\mathrm{dy}}$ as the function of mass flow flux of solution ($L$) was developed for the CELdek 5090 type packing in this study using the conventional volumetric method [28], i.e. $\overline{M}_{\mathrm{dy}}$ is equal to 27.8$L$. $\overline{M}_{\mathrm{dy}}$ is in positive correlation with the mass flow flux of solution, which is consistent with the results obtained in the study [25].

$$M_{\mathrm{dy}} = AH\overline{M}_{\mathrm{dy}} \tag{18}$$

$M_{\mathrm{a}}$ is the total mass of air in the dehumidifier which can be calculated by Eq. (19).

$$M_{\mathrm{a}} = \rho_{\mathrm{a}}\varepsilon_{\mathrm{a}}AH \tag{19}$$

The total volume of the packed tower is occupied by the packing material, the air and the solution. The volume fraction of the air ($\varepsilon_{\mathrm{a}}$) in the packing can be calculated by Eq. (20).

$$\varepsilon_{\mathrm{a}} + \varepsilon_{\mathrm{s}} + \varepsilon_{\mathrm{p}} = 1 \tag{20}$$

In Eq. (20), the volume fraction of the packing ($\varepsilon_{\mathrm{p}}$) can be provided by manufacturer. The volume fraction of the desiccant ($\varepsilon_{\mathrm{s}}$) is calculated by Eq. (21).

$$\varepsilon_{\mathrm{s}} = \frac{M_{\mathrm{s}}}{\rho_{\mathrm{s}}AH} \tag{21}$$

When calculating *NTU*, the wetted specific surface area of the packing ($a_{\mathrm{w}}$) and the mass transfer coefficient ($k_{\mathrm{m}}$) are the two parameters to be identified. $a_{\mathrm{w}}$ refers to the effective mass transfer area between the desiccant and the air. The correlation of $a_{\mathrm{w}}$ was given by Fumo *et al.* [29]. According to the correlation, the surface energy of packing materials, the surface tension of liquid desiccant [29], as well as the superficial flow rate of desiccant solution [29, 30] are found as the main influence factors of $a_{\mathrm{w}}$. The heat and mass transfer coefficients are varied by different experimental conditions. Table 1 summarizes typical empirical correlations for the heat and mass transfer coefficients which are available in literature. The details of the dehumidifiers and the operating conditions can be found in literature [27, 31, 32]. As there are still a lack of empirical correlations of heat and mass transfer coefficients for the packing adopted in this research, new empirical correlations should be developed. Firstly, experimental values of heat and mass transfer coefficients were determined by using the method proposed by Yin and Zhang [31]. Then the empirical correlations of heat and mass transfer coefficients were developed by dimensionless analysis, as shown at the bottom of Table 1. A total of 62 sets of experimental data were used for developing the new correlations. The validation ranges of the new correlations are given Table 2, and the average deviations between the calculated values by using the new correlations and the experimental data are within 15% for both correlations. The real driven force of mass transfer (i.e. the water vapor partial pressure difference between air and solution surface) is used in the new correlations instead of only the desiccant concentration in other correlations (Chung *et al.* [32]). It means the new correlations have better applicability. When the heat and mass transfer coefficients are obtained from the empirical correlations, the Lewis number can be determined by Eq.(5) and *NTU* can be determined by Eq.(6).

Table 1
The empirical correlations for heat and mass transfer coefficients.

| Author | Correlation | Type of packing | Desiccant |
|---|---|---|---|
| Chung *et al.* [32] | $Sh = 1.326 \times 10^{-4}\ Re^{1.16}\ Sc^{0.333}(1-X)^{-0.94}(\frac{L}{G})^{0.27}$<br>$Nu = 5.20 \times 10^{-5}\ Re^{1.6}\ Pr^{0.333}(1-X)^{1.56}(\frac{L}{G})^{0.50}$ | Polypropylene random packing | LiCl |
| Chung *et al.* [32] | $Sh = 2.25 \times 10^{-4}\ Re^{1.0}\ Sc^{0.333}(1-X)^{-0.75}(\frac{L}{G})^{0.10}$<br>$Nu = 2.78 \times 10^{-6}\ Re^{1.6}\ Pr^{0.333}(1-X)^{1.8}(\frac{L}{G})^{0.40}$ | Cellulose structured packing | LiCl |
| Al.Farayedhi *et al.* [27] | $K_m a = 0.55\, u_s{}^{0.1}\ u_a{}^{0.79} exp\ (-0.0293 T_a)$<br>$K_a a = 13.0\, u_s{}^{0.1}\ u_a{}^{0.79} exp\ (-0.026 T_a)$ | Gauze-type structured packing | LiCl |
| Yin and Zhang [31] | $K_m = 3.0223 \times 10^{-4} u_a{}^{0.7407} \omega_a exp(-0.057101 T_a)$ $exp(-0.0011294 T_s)^{2.1505}\ exp\ (19.377 X_s)$<br>$K_a = 6.834 \times 10^{6}\ u_a{}^{1.3}\ T_a{}^{-3.9} \omega_a{}^{2.2}\ T_s{}^{-1.2}$ $exp(-5.71 \times 10^{-2} T_a)\ exp(-9.28 \times 10^{-2} \omega_a)$ $exp(-1.13 \times 10^{-3} T_s)\ exp(6.68 X_s)$ | CELdek 7090 | LiCl |
| Present study | $Sh = 0.034 Re^{0.77} Sc^{0.33}(\frac{P_a - P_s}{P_0})^{0.13}(\frac{L}{G})^{0.3}$<br>$Nu = 0.028\, Re^{0.9}\ Pr^{0.33}(\frac{L}{G})^{0.51}$ | CELdek 5090 | LiCl |

Table 2

Validation ranges of the operating parameters for the present correlations.

| $m_a$ (kg/s) | $T_{a,in}$ (ºC) | $\omega_{a,in}$ (g/kg) | $m_s$ (kg/s) | $T_{s,in}$ (ºC) | $\xi$ (%) |
|---|---|---|---|---|---|
| 0.048-0.082 | 25.0-40.5 | 11.6-25.1 | 0.050-0.120 | 16.4-26.9 | 32.1%-40.1% |

**3. Experimental facility**

An adiabatic counter flow packed-type dehumidifier has been established for validating the proposed dynamic heat and mass transfer model. The schematic of the experimental facility is shown in Fig.4. The dehumidifier is a packed structure tower with the shell of acrylic plastic glazing. The structured packing (Munters CELdek 5090 Type) is adopted and its properties are shown in Table 3. This type of packing is made of porous cellulose material, which is a strong adsorbent for the desiccant solution. In addition, the capillary action also contributes to a better wettability for the porous packing [33]. Therefore, the total surface area of the packing can be considered completely wetted (i.e., $a_w = a$) [23].

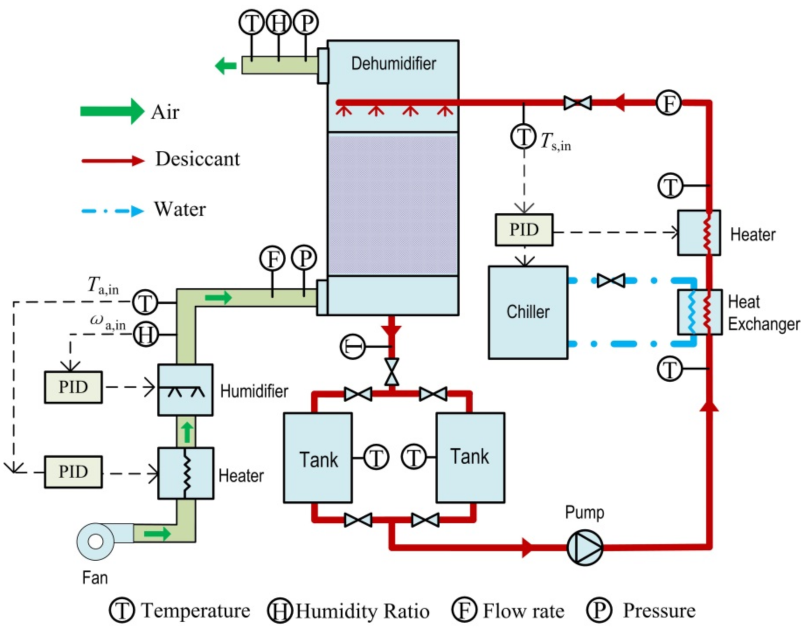


Fig. 4. Experimental facility.

Table 3

Properties of the structured packing.

| | |
|---|---|
| Specific surface area ($m^2/m^3$) | 650 |
| Density ($g/cm^3$) | 0.68 |
| Void fraction | 0.05 |
| Equivalent diameter (mm) | 6.0 |
| Length (m) | 0.3 |
| Width (m) | 0.3 |
| Height (m) | 0.4 |

An electric heater and an electrode humidifier are installed in the air duct. When the air flows through the duct, it is heated and humidified to the desired temperature and humidity ratio. The desiccant solution with the desired inlet concentration is prepared in advance and stored in the strong solution tank. The desiccant solution with a constant concentration is then pumped by a fluorine-lining magnetic pump from the strong solution tank to a heat exchanger and an electric heater for cooling or heating to obtain the desired temperature. The cooling water in the heat exchanger is generated by a chiller. When the desired conditions of the air and the desiccant are reached, the desiccant then flows into the dehumidifier. Two spray heads (each with ten holes below) and a porous plate are used in distributing the desiccant uniformly over the packing. After heat and mass transferred with the counter flow air, the diluted desiccant solution flows from the dehumidifier into the week solution tank. For preparing the next experiment, the functions of the two solution tanks can be switched by the four valves between them, and the desiccant solution with the desired inlet concentration needs to be prepared as the strong solution once more.

The inlet and outlet states of the air and the desiccant can be measured during the entire dehumidification process. The temperatures of the air and the desiccant solution are measured by fast-response type PT100 RTDs. Two humidity transducers are used to measure the inlet and outlet air humidity ratios. The flow rates of the air and the desiccant solution are measured by a differential pressure flow meter and an electromagnetic flow meter, respectively. The desiccant solution concentration can be calculated based on the measured solution temperature and density (by a specific gravity hydrometer). The fitting formulas used for calculating thermophysical properties of LiCl aqueous solution are reported by Conde [34]. By using two PID temperature controllers, the temperature of the air and the desiccant are maintained at two fixed set-points, respectively. The air humidity is maintained at constant by a PID humidity controller. All the measured data are collected by the data acquisition unit (Agilent 34972A). More details about the measuring instruments and the uncertainty analysis of the experiments can be seen in literature [35].

## 4. Results and discussions

### *4.1. Model validation under transient working conditions*

Two experiment cases were conducted for validating the dynamic model.

The first case studies the dynamic characteristics at the beginning of a dehumidification process, which simulates the dehumidifier starts to work either for the first time, or after a period of idle. First, the air with the desired inlet condition flows into the dehumidifier for a few minutes. Then, the desiccant solution with the desired inlet condition flows into the dehumidifier, and the dehumidification experiment begins. The inlet conditions of the air and the desiccant solution, which are listed as Case 1 in Table 4, keep unchanged during the test.

The second case studies the dynamic dehumidification process when the inlet solution temperature changes linearly. The desiccant solution temperature is a critical factor that influences the dehumidification performance. In the practical application of the liquid desiccant systems, the desiccant solution temperature often changes continually, therefore it is necessary to study the dynamic characteristics of the dehumidifier when the desiccant solution temperature changes. The inlet conditions of the air and the desiccant solution are listed as Case 2 in Table 4. Fig.5 shows the measured inlet solution temperature over time. The inlet solution temperature changes from 22.5 $^{o}$C to 18.3 $^{o}$C (from 70s to 300s). When conducting the numerical study, a steady-state model of the liquid desiccant dehumidifier developed by Chen *et al.* [15] is introduced in comparison with the proposed dynamic model.

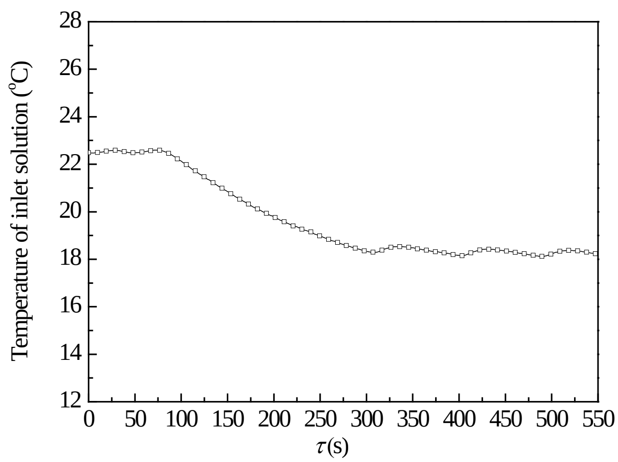


Fig. 5. The measured temperature of inlet solution under linear variation condition.

Table 4
Inlet conditions of air and desiccant solution in experiments.

| | Air | | | Desiccant solution | | |
|---|---|---|---|---|---|---|
| | $m_{a}$ (kg/s) | $T_{a}$ (ºC) | $\omega_{a}$ (g/kg) | $m_{s}$ (kg/s) | $T_{s}$ (ºC) | $\xi$ |
| Case 1 | 0.0814 | 30.0 | 15.4 | 0.1179 | 20.8 | 36.2% |
| Case 2 | 0.0630 | 30.0 | 18.2 | 0.0976 | 22.5-18.3 | 34.8% |

Besides the two important model outputs, i.e., the outlet air humidity ratio and the outlet air temperature, two popular indices for evaluating the performance of a liquid desiccant dehumidification process [29], i.e., the dehumidification rate ($m_{de}$) and the dehumidification effectiveness ($\eta$), are adopted in this study to compare the model with experiment. The dehumidification rate refers to the moisture removed from the air per unit time, as shown in Eq. (22). The dehumidification effectiveness is defined as the ratio between the real dehumidification ability and the maximum possible dehumidification ability, as shown in Eq. (23).

$$m_{\mathrm{de}} = m_{\mathrm{a}}(\omega_{\mathrm{a,in}} - \omega_{\mathrm{a,out}}) \tag{22}$$

$$\eta = \frac{\omega_{\mathrm{a,in}} - \omega_{\mathrm{a,out}}}{\omega_{\mathrm{a,in}} - \omega_{\mathrm{e,in}}} \tag{23}$$

where, $\omega_{e,in}$ is the equivalent humidity ratio of the inlet solution. For the adiabatic-type dehumidifier, the maximum dehumidification effectiveness can be obtained when the outlet air is in equilibrium with the inlet desiccant solution.

In order to evaluate the accuracy of the proposed model, two error indices, Root-Mean-Square Error (RMSE) and Mean Absolute Error (MAE), are used.

$$RMSE = \sqrt{\frac{\sum_{i=1}^{N}(\theta_{\mathrm{Num}} - \theta_{\mathrm{Exp}})^2}{N}} \tag{24}$$

$$MAE = \frac{\sum_{i=1}^{N}|\theta_{\mathrm{Num}} - \theta_{\mathrm{Exp}}|}{N} \tag{25}$$

where $\theta$ represents the outlet air humidity ratio, the outlet air temperature, the dehumidification rate or the dehumidification effectiveness; $N$ is the sample of the dynamic data (e.g., one sampling point per second in both numerical solution and experiment).

*4.1.1. Case 1：Dynamic characteristics at the beginning of a dehumidification process*

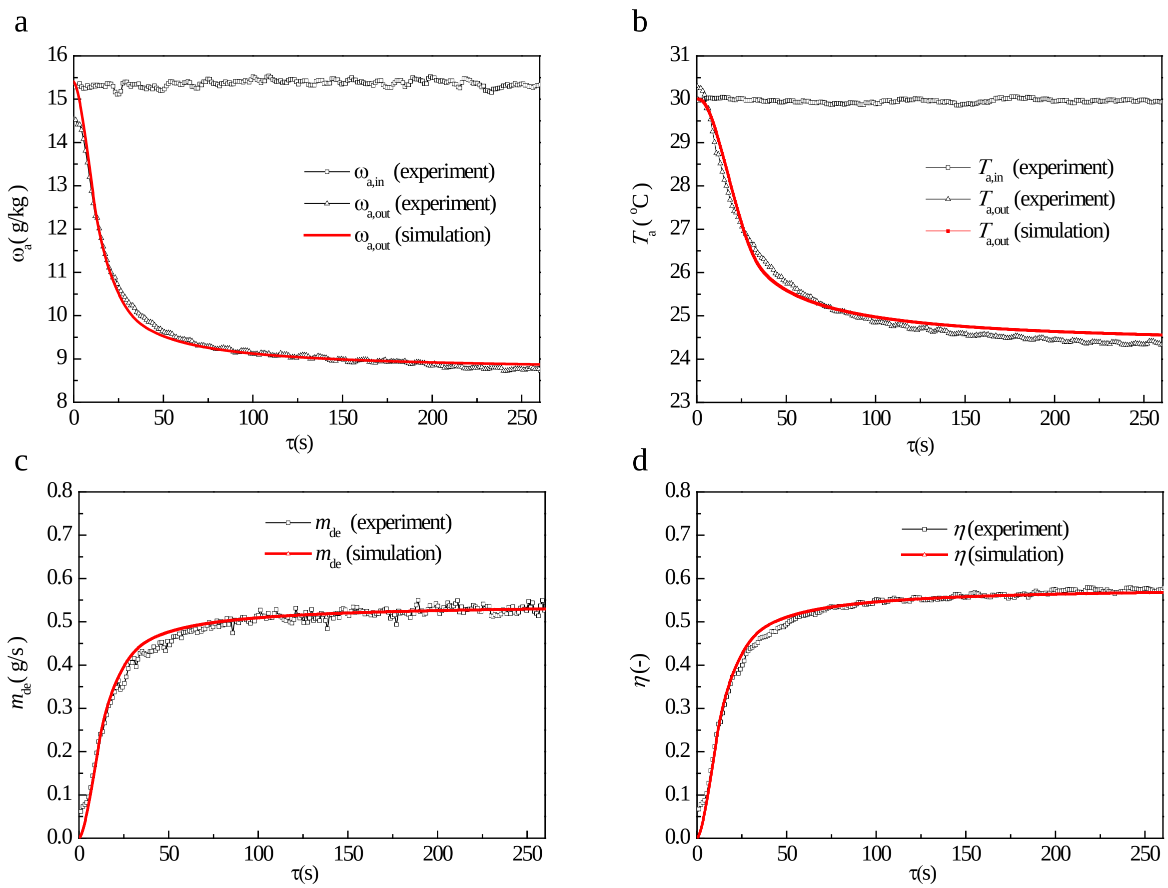


Fig. 6. Comparison between numerical results and experimental results (Case 1): (a) outlet air humidity ratio, (b) outlet air temperature, (c) dehumidification rate and (d) dehumidification effectiveness.

Fig. 6 compares the numerical results with the experimental results of the four indices, i.e., (a) outlet air humidity ratio, (b) outlet air temperature, (c) dehumidification rate and (d) dehumidification effectiveness. It can be found that the numerical results show good agreement with the experimental results. The RMSE and MAE are shown in Table 5. The RMSE is less than 0.2g/kg for the outlet air humidity ratio, 0.2°C for the outlet air temperature, less than 0.02g/s for the dehumidification rate and less than 2% for the dehumidification effectiveness, respectively. The MAEs are even smaller for all of the performance indices. It is proved that the model can be used in predicting the dynamic heat and mass transfer characteristics of the dehumidification process. Fig. 6 also reveals that the outlet air humidity ratio and temperature decrease over time while the dehumidification rate and the dehumidification effectiveness increase over time.

It also can be observed in Fig. 6 that the experimental outlet air humidity ratio and temperature are not equal to the experimental inlet air humidity ratio and temperature at the initial period. That is because there is a few amount of desiccant stored in the packing before this experiment. The air should be dehumidified and heated to a quasi-steady state first. Thus, the experimental outlet air humidity ratio is a little lower than the inlet air humidity ratio, while the experimental outlet air temperature is a little higher than the inlet air temperature.

Table 5
The Root-Mean-Square Error (RMSE) and Mean Absolute Error (MAE) of outlet air humidity ratio and temperature, dehumidification rate and dehumidification effectiveness for different case studies.

| | | RMSE | | | | MAE | | | |
|---|---|---|---|---|---|---|---|---|---|
| | | $\omega_{a,out}$ (g/kg) | $T_{a,out}$ (°C) | $m_{de}$ (g/s) | $\eta$ (-) | $\omega_{a,out}$ (g/kg) | $T_{a,out}$ (°C) | $m_{de}$ (g/s) | $\eta$ (-) |
| Case 1 | Dynamic model | 0.192 | 0.207 | 0.018 | 0.017 | 0.159 | 0.190 | 0.014 | 0.014 |
| Case 2 | Dynamic model | 0.062 | 0.108 | 0.005 | 0.005 | 0.050 | 0.081 | 0.004 | 0.004 |
| | Steady-state model | 0.113 | 0.270 | 0.008 | 0.009 | 0.095 | 0.219 | 0.007 | 0.007 |

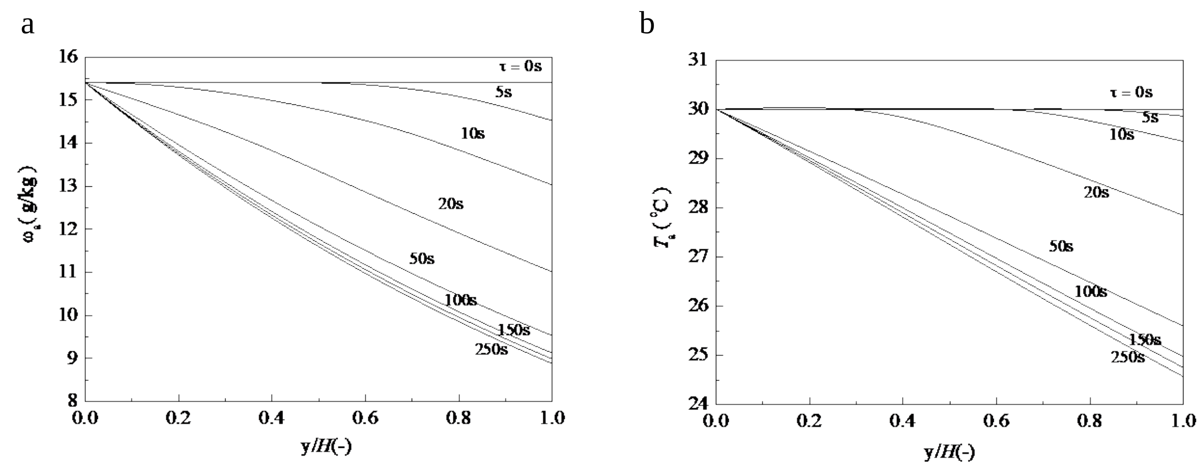


Fig. 7. Dynamic distributions of (a) air humidity ratio and (b) air temperature along the vertical flow path.

Using the proposed dynamic model, the transient distributions of the air humidity ratio and temperature along the vertical flow path are also investigated numerically. Fig. 7 shows the numerical results of the transient distributions along the vertical flow path. It can be observed that both the air humidity ratio and temperature decrease along the flow direction. The changing trend of the air temperature is similar to that of the air humidity ratio, which indicates that the heat transfer and mass transfer are coupled and they influence each other. It cost about 250 seconds to achieve steady states for the air humidity ratio and temperature. Actually, there are little changes of the air states after 150 seconds.

*4.1.2. Case 2：Dynamic characteristics under the condition of linear variation of inlet solution temperature*

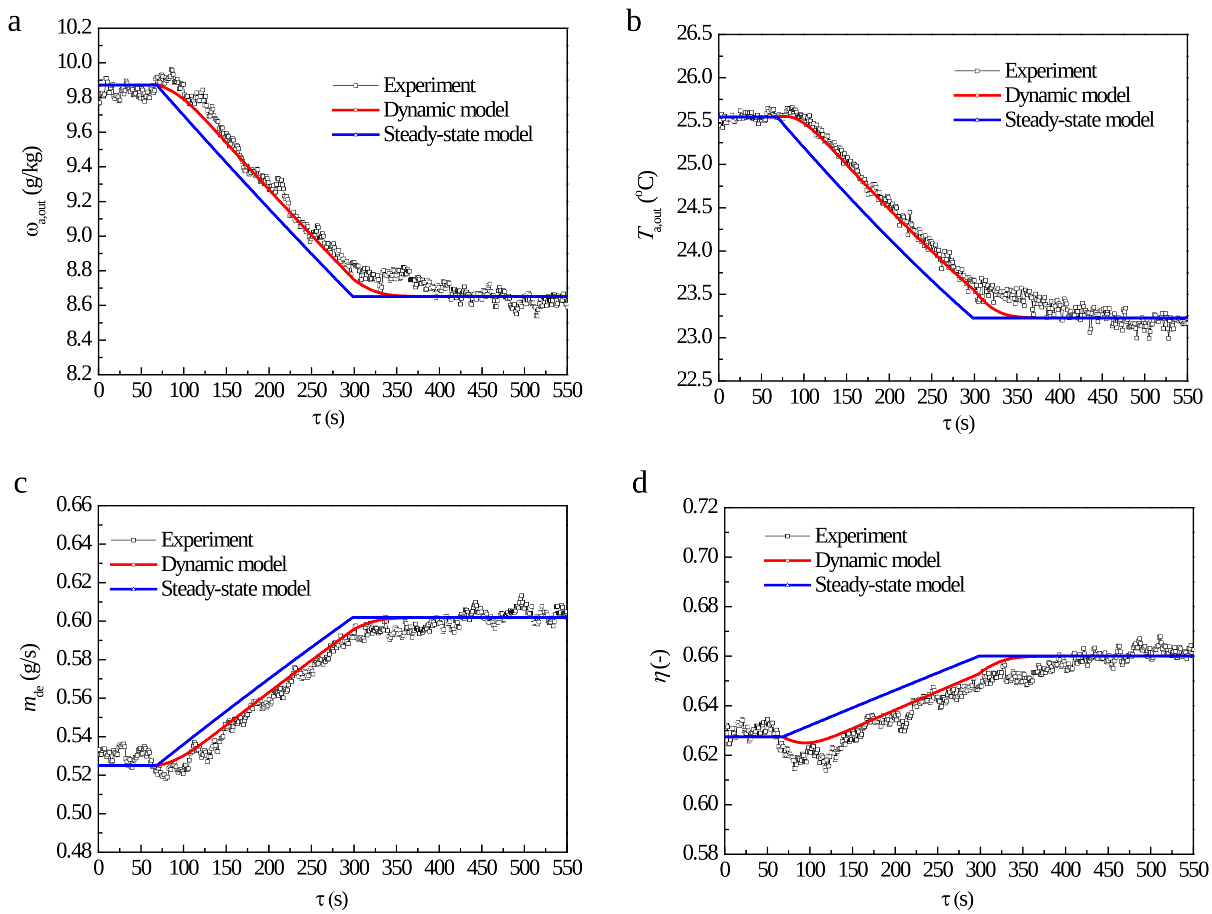


Fig. 8. Comparisons between numerical results and experimental results (Case 2): (a) outlet air humidity ratio, (b) outlet air temperature, (c) dehumidification rate and (d) dehumidification effectiveness.

Fig.8 compares the experimental results with the numerical results from the steady-state and dynamic models, respectively. During the linear change (70s to 300s) of the inlet solution temperature, the results of the dynamic model show a better agreement with the experimental data. The results of the steady-state model change faster than the experimental results. The numerical results of these two models are almost the same at the initial period (before 70s) and the last steady period (after 400s), which indicates that the proposed dynamic model converges to the steady state model described above and also can predict the dehumidification performance when the outlet conditions of the air and the desiccant solution reach the steady states. The fluctuation of the experimental results is mainly caused by the transient fluctuation effects of inlet variables of the air and the desiccant solution. The Root-Mean-Square Error and Mean Absolute Error for the numerical results of the two models are also shown in Table 5. It shows that the RMSE and MAE of the dynamic model are very small, while the RMSE and MAE of the steady-state model are almost twice than that of the dynamic model. For a longer period of the dehumidification process, the inlet conditions of the air and the desiccant solution may be continually varied with time, they still can be set as the inputs of the model and the performance of dehumidifier also can be predicted by the proposed dynamic model.

### *4.2. Sensitivity analysis of thermal mass on dehumidifier dynamics*

The thermal capacity of the dehumidifier is the major factor influencing the dynamic characteristics of the dehumidifier. The dynamic characteristics of the dehumidifier can be quantified by the time constant of the dynamic response. The time constant ($\tau_c$) is defined as the time when an outlet variable approaches 63.2% of the difference between the initial steady state and the final steady state [36], which can be calculated by Eq. (26).

$$\boldsymbol{\Phi}(\boldsymbol{\tau_c}) = \boldsymbol{\Phi}(\boldsymbol{i}) - \mathbf{0.632}(\boldsymbol{\Phi}(\boldsymbol{i}) - \boldsymbol{\Phi}(\boldsymbol{f})) \quad (26)$$

where $\boldsymbol{\Phi}$ represents an outlet variable (i.e. outlet air temperature or outlet air humidity ratio), $\tau_c$ represents time constant, *i* represents initial steady state, *f* represents final steady state.

According to the analysis in Section 2, the thermal capacity of the dehumidifier consists of the thermal mass of the air, the desiccant solution and the packing in the dehumidifier, especially the latter two. The thermal mass of the packing is the dry weight of the packing ($M_p$). The thermal mass of the desiccant solution held in the dehumidifier can be divided into the static desiccant solution ($M_{st}$) and the dynamic desiccant solution ($M_{dy}$) held in the dehumidifier. Sensitivity analysis is conducted to investigate the effects of the thermal mass on the dehumidifier dynamics. Take Case 1 in Section 4.1 as the reference case, the dynamic responses of the dehumidifier are simulated when the values of the three types of thermal mass vary separately. The varying ranges should be set reasonably. The thermal mass of the packing is mainly determined by the density of parking materials. As the density of the reference packing material (i.e., CELdek

5090 used in the experiment as well) is very small, the ratio of the packing thermal mass used in the sensitivity analysis changes between 0 and 10, in which 0 means the packing thermal mass is neglected and 10 means the packing thermal mass is 10 times that of the reference packing. The mass of the static desiccant solution ($M_{st}$) is constrained by the volume fraction ($\varepsilon_p$) and material of the packing and it cannot be very large (e.g., for the packing made of metal, $M_{st}$ can be neglected [27]).The mass of the static desiccant solution ($M_{st}$) used in the sensitivity analysis changes between -100% and +10% of the reference value. The thermal mass of the dynamic desiccant solution ($M_{dy}$) used in the sensitivity analysis changes between -50% and +50% of the reference value. Apart from the thermal mass, the working conditions and heat and mass transfer coefficients are assumed to be unchanged.

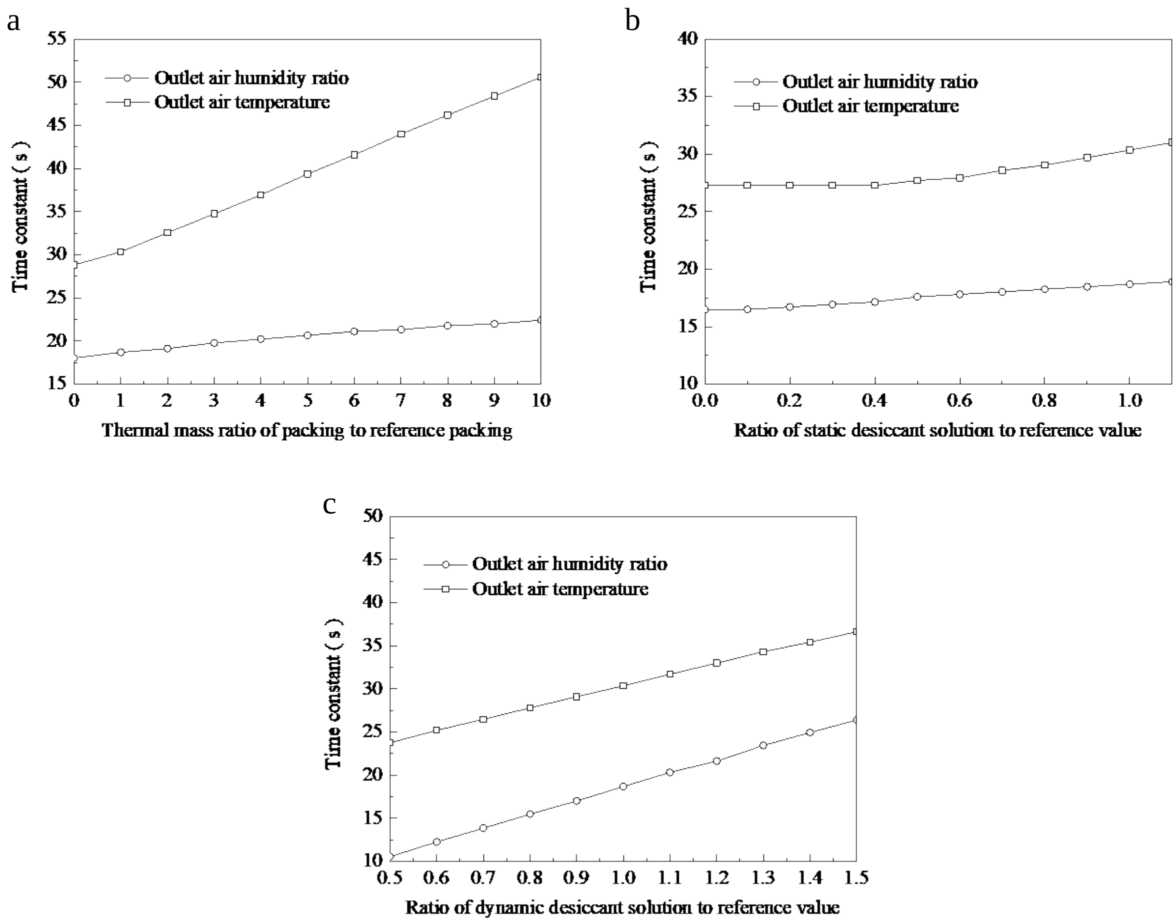


Fig. 9. The influence of (a) thermal mass of packing, (b) static desiccant solution and (c) dynamic desiccant solution on the time constant of outlet air.

Fig.9 shows the simulation results using the dynamic model when the three types of thermal mass change separately. A general trend can be seen that the time constants increase with the increase of thermal mass, which agrees with the physical principles. Among the three types of thermal mass, the effect of the dynamic desiccant solution is the most significant. Fig.9 (a) indicates that the thermal mass of the packing has obvious influence on the time constant of the outlet air temperature, while its influence on the outlet air humidity ratio is smaller. The function of the static desiccant solution for the dynamic response of the dehumidifier is similar to the packing, which only conducts the heat transfer. The results from Fig.9 (b) demonstrate that the static desiccant solution has little influence on the dynamic response of the dehumidifier. For the packing which is the porous media or hydrophilic material, it usually has more static desiccant solution stored in it and therefore has a good surface wetness, while without obviously increasing the dynamic response time of the dehumidifier. The results in Fig.9 (c) show that the dynamic desiccant solution has a significant influence on the dynamic response of the dehumidifier. Both of the time constants of the outlet air humidity ratio and temperature decrease obviously when $M_{\mathrm{dy}}$ is reduced. One main factor influencing the value of $M_{\mathrm{dy}}$ is the film thickness of desiccant solution on the packing surface. They are the positive correlation. Therefore, a thin film thickness results in a quick dynamic response of the dehumidifier. Reducing the film thickness is a feasible method to reduce the response time of the dehumidifier. For a given flow rate of the desiccant solution, the film thickness is influenced by the flow channel configuration of the packing, the solution distribution pattern and the physical properties of the solution [27]. In addition, the excessive height of packing results in the accumulation of the desiccant solution and then enlarges the film thickness [35].

Besides, it also can be found from Fig.9 that the time constants of the outlet air humidity ratio are always smaller than that of the outlet air temperature, which are consistent with the experimental findings [36]. It means the mass transfer reaches to the steady state always faster than the heat transfer in the dehumidifier. Due to the small scale and small thermal capacity of the reference dehumidifier, the time constants of the outlet air are not significant. However, the developed model and the simulation results in this study are generic and can be used as the design guideline for the controller of the liquid desiccant dehumidifier.

## Conclusions

This paper presents a new mathematical model for characterizing the dynamic dehumidification process in the counter flow packed-type liquid desiccant dehumidifier. Convenient approaches to quantifying the thermal mass of the packing and the desiccant solution held in the dehumidifier are proposed, which are essential parameters of the dynamic model. The thermal mass of the packing can be easily quantified using the density and specific heat of the packing material, the actual volume of the packing tower and the volume fraction of the packing. The desiccant solution held in the dehumidifier includes both the static and dynamic components. The former can be quantified by the data provided by the manufacturers or by weighing a piece of packing material before and after soaking it in the solution. The latter can be quantified by using the conventional volumetric method.

The dynamic model is validated by the experiments of two case studies. A steady-state model of the liquid desiccant dehumidifier from the existing literature is also introduced for comparisons. The transient working conditions in the two cases are: at the beginning of a dehumidification process (Case 1), the linear variation conditions of the inlet solution temperature (Case 2). These transient working conditions represent the start and continuous operation stages of the dehumidifier, respectively. The results prove that the numerical results of the dynamic model show a good agreement with the experimental results in the two cases. The dynamic model can predict the transient process accurately and timely. It is also suitable for integrating with other air conditioning components for system dynamic simulation and testing control methods of the liquid desiccant hybrid air conditioning systems.

Using the dynamic model developed, sensitivity analysis of the thermal capacity of the dehumidifier on the dehumidifier dynamics is conducted. Time constants of the outlet air humidity ratio and temperature are calculated for comparing the dynamic response of the dehumidifier with different thermal mass. The results show that the thermal mass of the packing has a significant influence on the time constant of the outlet air temperature while has only small influence on that of the outlet air humidity ratio. The static desiccant solution held in the dehumidifier has little influence on the dynamic response of the dehumidifier. By contrast, the dynamic desiccant solution held in the dehumidifier has a more significant effect on the dehumidifier dynamics. Quicker response of the dehumidifier can be achieved when the dynamic desiccant solution is reduced. The sensitivity analysis results are helpful for the configuration optimization and controller design of the liquid desiccant dehumidifier.

**Acknowledgement**

The research work presented in this paper was financially supported by the National Natural Science Foundation of China (No.51306157) and the Research Grant Council (RGC) of the Hong Kong SAR (GRF/5300/11E).

**References**

[1] L.Z. Zhang, F. Xiao, Simultaneous heat and moisture transfer through a composite supported liquid membrane, International Journal of Heat and Mass Transfer 51 (9-10) (2008) 2179-2189.

[2] R.M. Lazzarin, F. Castellotti, A new heat pump desiccant dehumidifier for supermarket application, Energy and Buildings 39 (2007) 59-65.

[3] X.F. Niu, F. Xiao, Z.J. Ma, Investigation on capacity matching in liquid desiccant and heat pump hybrid air-conditioning systems, International Journal of Refrigeration 35 (2012) 160-170.

[4] T. Zhang, X.H. Liu, Y. Jiang, Performance optimization of heat pump driven liquid desiccant dehumidification systems, Energy and Buildings 52 (2012) 132-144.

[5] S. Alizadeh, Performance of a solar liquid desiccant air conditioner-An experimental and theoretical approach, Solar Energy 82 (2008) 563-572.

[6] Y.G. Yin , B.J. Zheng, C. Yang, X.S. Zhang, A proposed compressed air drying method using pressurized liquid desiccant and experimental verification, Applied Energy 141 (2015) 80-89.

[7] G.M. Ge, F. Xiao, X.F. Niu, Control strategies for a liquid desiccant air-conditioning system, Energy and Buildings 43 (2011) 1499-1507.

[8] F. Xiao, G.M. Ge, X.F. Niu, Control performance of a dedicated outdoor air system adopting liquid desiccant dehumidification, Applied Energy 88 (2011) 143-149.

[9] Q. Ma, R.Z. Wang, Y.J. Dai, X.Q. Zhai, Performance analysis on a hybrid air-conditioning system of a green building, Energy and Buildings 38 (2006) 447-453.

[10] W.F. Zhu, Z.J. Li, S. Liu, S.Q. Liu, Y. Jiang, In situ performance of independent humidity control air-conditioning system driven by heat pumps, Energy and Buildings 42 (2010) 1747-1752.

[11] K. Zhao, X.H. Liu, T. Zhang, Y. Jiang, Performance of temperature and humidity independent control air-conditioning system in an office building, Energy and Buildings 43 (2011) 1895-1903.

[12] X.F. Niu, F. Xiao, G.M. Ge, Performance analysis of liquid desiccant based air-conditioning system

under variable fresh air ratios, Energy and Buildings 42 (12) (2010) 2457-2464.

[13] R.E. Treybal, Adiabatic gas absorption and stripping in packed towers, Industrial and Engineering Chemistry 61(7) (1969) 36-41.

[14] A.Y. Khan, H.D. Ball, Development of a generalized model for performance evaluation of packed-type liquid sorbent dehumidifiers and regenerators, ASHRAE Transactions 98 (1992) 525-533.

[15] X.Y. Chen, Z. Li, Y. Jiang , K.Y. Qu, Analytical solution of adiabatic heat and mass transfer process in packed-type liquid desiccant equipment and its application, Solar Energy 80 (2006) 1509-1516.

[16] X.H. Liu, Y. Jiang, J.J. Xia, X.M. Chang, Analytical solutions of coupled heat and mass transfer processes in liquid desiccant air dehumidifier/regenerator, Energy Conversion and Management 48 (2007) 2221-2232.

[17] D. Babakhani, M. Soleymani, An analytical solution for air dehumidification by liquid desiccant in a packed column, International Communications in Heat and Mass Transfer 36 (2009) 969-977.

[18] D.I. Stevens, J.E. Braun, S.A. Klein, An effectiveness model of liquid-desiccant system heat/mass exchangers, Solar Energy 42 (6) (1989) 449-455.

[19] X.L. Wang, W.J. Cai , J.G. Lu , Y.X. Sun, X.D. Ding, A hybrid dehumidifier model for real-time performance monitoring, control and optimization in liquid desiccant dehumidification system, Applied Energy 111 (2013) 449-455.

[20] S.W. Peng, Z.M. Pan, Heat and mass transfer in liquid desiccant air-conditioning process at low flow conditions, Communication Nonlinear Science Numerical Simulation 14 (2009) 3599-3607.

[21] R. Namvar, G.M. Ge, C.J. Simonson, R.W. Besant, Transient heat and moisture transfer characteristics of a liquid-to-air membrane energy exchanger (LAMEE) model verification and extrapolation, International Journal of Heat and Mass Transfer 66 (2013) 757-771.

[22] Y.M. Luo, H.X. Yang, L. Lu, Dynamic and microscopic simulation of the counter-current flow in a liquid desiccant dehumidifier, Applied Energy 136 (2014) 1018-1025.

[23] S.V. Potnis, T.G. Lenz, Dimensionless mass-transfer correlations for packed-bed liquid-desiccant contactors, Industrial & Engineering Chemistry Research 35 (1996) 4185-4193.

[24] J.A. Rocha, J.L. Bravo, J. R. Fair, Distillation columns containing structured packings: a comprehensive model for their performance. 1. Hydraulic Models, Industrial & Engineering Chemistry Research 32

(1993) 641-651.

[25] R.H. Weiland, K.R. Ahlgren, M. Evans, Mass-transfer characteristics of some structured packings, Industrial & Engineering Chemistry Research 32 (1993) 1411-1418.

[26] M. Seyed-Ahmadi, B. Erb, C.J. Simonson, R.W. Besant, Transient behavior of runaround heat and moisture exchanger system. Part I: Model formulation and verification, International Journal of Heat and Mass Transfer 52 (2009) 6000-6011.

[27] A.A. Al-Farayedhi, P. Gandhidasan, M.A. Al-Mutairi, Evaluation of heat and mass transfer coefficients in a gauze-type structured packing air dehumidifier operating with liquid desiccant, International Journal of Refrigeration 25 (2002) 330-339.

[28] P. Suess, L. Spiegel, Hold-up of Mellapak structured packings, Chemical Engineering and Processing, 31 (1992) 119-124

[29] N. Fumo, D.Y. Goswami, Study of an aqueous lithium chloride desiccant system: air dehumidification and desiccant regeneration, Solar Energy 72(4) (2002) 351-61.

[30] M.H. Brito, U.V. Stockar, A.M. Bangerter, P. Bomio, and M. Laso, Effective mass-transfer area in a pilot plant column equipped with structured packings and with ceramic rings, Industrial & Engineering Chemistry Research 33 (1994) 647-656.

[31] Y.G. Yin, X.S. Zhang, A new method for determining coupled heat and mass transfer coefficients between air and liquid desiccant, International Journal of Heat and Mass Transfer 51 (2008) 3287-3297.

[32] T.W. Chung, T.K. Ghosh, A.L. Hines, Comparison between random and structured packings for dehumidification of air by lithium chloride solutions in a packed column and their heat and mass transfer correlations, Industrial & Engineering Chemistry Research 35(1) (1996) 192-198.

[33] G. Q. Wang, X. G. Yuan, K. T. Yu, Review of mass-transfer correlations for packed columns, Industrial & Engineering Chemistry Research 44 (2005) 8715-8729.

[34] M.R. Conde, Properties of aqueous solutions of lithium and calcium chlorides: formulations for use in air conditioning equipment design, International Journal of Thermal Sciences 43(4) (2004) 367-382.

[35] L.S. Wang, F. Xiao, X.J. Zhang, R. Kumar, An experimental study on the dehumidification performance of a counter flow liquid desiccant dehumidifier, International Journal of Refrigeration 70 (2016) 289-301.

[36] R. Namvar, D. Pyra, G.M. Ge, C.J. Simonson, R.W. Besant, Transient characteristics of a liquid-to-air membrane energy exchanger (LAMEE) experimental data with correlations, International Journal of Heat and Mass Transfer 55 (23-24) (2012) 6682-6694.